

Rigorous Potential Models of the Nucleon-Nucleon Force

Brian Sabbey

Department of Physics, Cornell University, Ithaca, NY 14853

Abstract

Rigorous potential models of the nucleon-nucleon force can be derived using renormalization techniques. I wrote a program in C to implement such a model. I used this program to calculate several properties of nucleon-nucleon interactions to demonstrate the usefulness of this model.

Background

Calculating properties of nucleon-nucleon interactions using QCD can be very computationally intensive or impossible. On the other hand, calculations that treat nucleons as elementary particles are not very accurate. This paper describes a method of efficiently including QCD effects while continuing to treat nucleons as elementary particles.[1]

This method for including complicated QCD effects is analogous to the classical electrodynamics method of approximating a complicated current source by a multipole expansion. At sufficient distance, this is an accurate approximation if the size of the current source is much smaller than the wavelength of the emitted radiation. In general, a probe of wavelength Λ can not resolve details of a structure that is a size much smaller than Λ .

In the nucleon-nucleon case, the “details” are the effects caused by the quark structure of the nucleons. This structure is ~ 1 -2 fm. So nucleons with $\Lambda > 2$ fm (momentum < 600 MeV) are insensitive to the exact QCD effects. Therefore the exact effects can be accurately replaced by simpler approximations of the effects.

A standard way to approximate short distance behavior is with a delta function added to the potential:

$$H = \frac{\mathbf{p}^2}{2m} + V(\mathbf{r}) + c\delta^3(\mathbf{r}) \quad (1)$$

The size of the delta function, c , is chosen to give a best fit to the data being modeled.

The Fourier transform of the potential makes it clear why a delta function will approximate short-distance behavior, and suggests how to extend the approximation. Because the potential is short-range, the Fourier transform, $\tilde{V}(q^2)$ will depend weakly on the transform variable, q^2 . Therefore, a Taylor expansion in q^2 will be a good approximation of the function:

$$\tilde{V}(q^2) = \tilde{V}(0) + q^2\tilde{V}'(0) + \dots \quad (2)$$

Transforming $\tilde{V}(0)$ back to coordinate space gives the delta function. Transforming higher powers of q^2 gives derivatives of the delta function. This suggests that a short-range potential with two “contact” terms,

$$V(\mathbf{r}) = c\delta^3(\mathbf{r}) + d\nabla^2\delta^3(\mathbf{r}), \quad (3)$$

will allow a better approximation. Now the two “coupling constants”, c and d , must be tuned to fit the data. Note that these parameters can be tuned to a single piece of data,

rather than a global fit. The lowest energy data is used for the tuning, since it contains the least error due to short-range effects.

The long range potential must also be included in the model. While the contact terms above can be tuned to model an arbitrary short-range potential, the long-range potential is specific to the system being modeled. For nucleons, the long range potential is due to the exchange of one or more pions. The potential due to the exchange of one pion, the largest contributor, is given by the Yukawa potential,

$$\frac{e^{-m_\pi r}}{r} \quad (4)$$

The exact form of the potential used in the calculations is given in the appendix. See Fig. 1 for typical potentials.

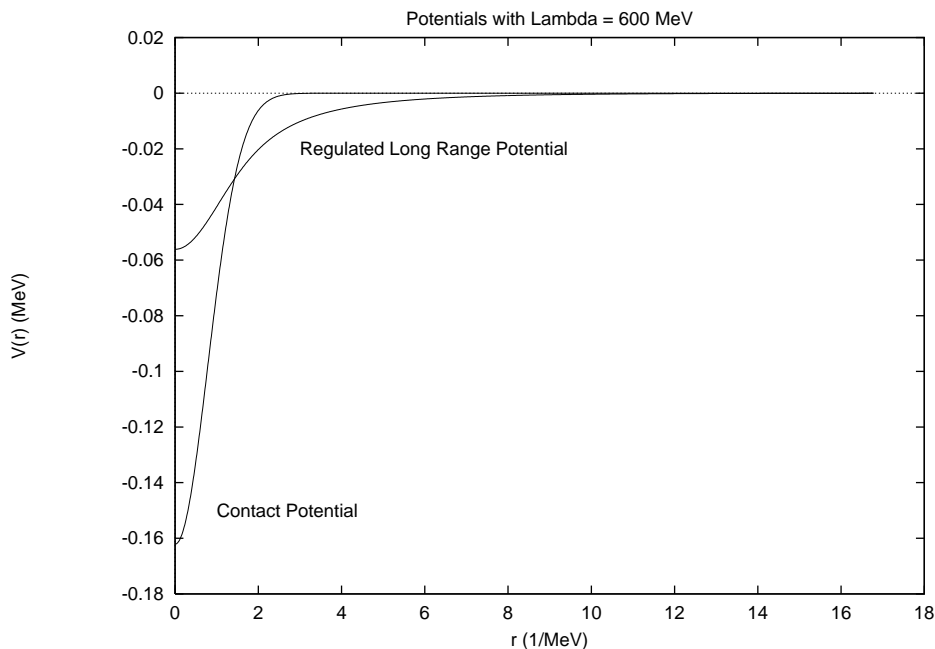


FIGURE 1. A typical regulated long-range potential, and a typical smeared delta function

Now the general short range potential and the long-range pion-exchange potential must be combined. The long-range potential needs to be regulated so that it will not have an effect on states of high momentum, for which the potential is incorrect. Regulating the potential is done by forcing the momentum-space form of the potential to zero for large values of the momentum. This can be done by multiplying the momentum-space form of the potential by something like $e^{-q^2/(2\Lambda^2)}$, where Λ is the *cutoff*—approximately the smallest value of the momentum excluded. The effect of these states will instead be included in the contact terms. The contact terms also need to be regulated to avoid infinities associated with the delta function. This is done by smearing the delta function over a finite distance:

$$\delta^3(\mathbf{r}) \rightarrow \delta_\Lambda^3(\mathbf{r}) \equiv \frac{\Lambda^3 e^{-r^2\Lambda^2/2}}{(2\pi)^{3/2}} \quad (5)$$

States with momentum greater than the cutoff are insensitive to the smearing of the delta function, in the same way that they are insensitive to the exact QCD effects. The smearing also regulates the delta function to exclude states with momentum $> \Lambda$. Fig. 1 shows a regulated long-range potential and a regulated delta function.

The accuracy of the model will depend on the value of Λ used. For too small a value, momentum states for which the long-range potential is accurate will be excluded, giving less accurate results. For too large a value of Λ , states are included that are sensitive to the short-range QCD effects that are not present in the model. This will not necessarily cause a decrease in accuracy, but it can make the contact terms difficult to find. The value for Λ for which the approximation stops improving then gives a good indication of the momentum at which the short-range effects become important.

The Calculations

I used this potential model with the Schrödinger equation to calculate properties of neutron-proton scattering, with total spin, j , one. These calculations were compared with data to determine their accuracy. [2]

The $j = 1$ case is more complicated than the $j = 0$ case because there is a coupling between the two ways of producing $j = 1$. The two ways are $l = 0$ (3S_1 state) with spin one and $l = 2$ (3D_1 state) also with spin one.

The data used most was the phase shift in neutron-proton scattering. The phase shift is the difference in phase between a free wave and a wave that interacts with a potential. The shift is measured at a point outside the range of the potential, where the waves both have the functional form of a free wave, but differ in phase. For example, an attractive potential will tend to “pull in” a wave, causing the wave to have a greater phase than a free wave.

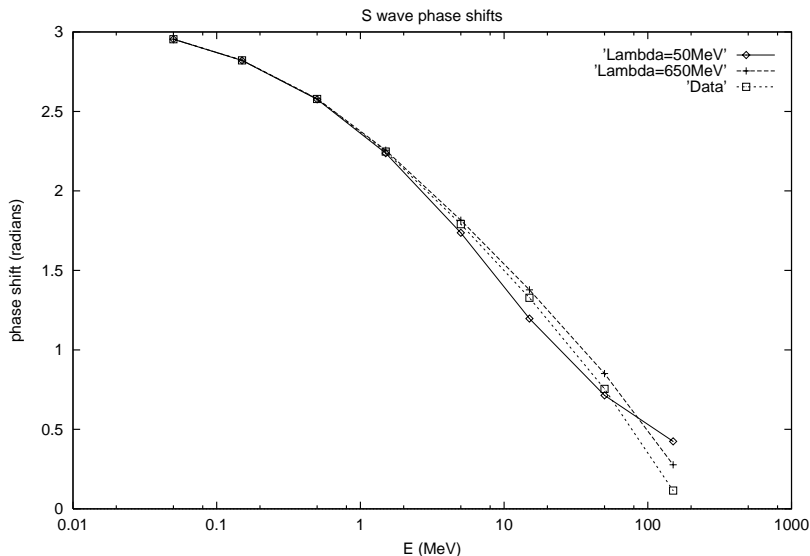


FIGURE 2. The 3S_1 phase shifts versus energy for two values of Λ . The data values are also shown.

Fig. 2 shows a plot of the calculated phase shift of the 3S_1 state versus energy for two values of the cutoff. A cutoff of 650 MeV is clearly more accurate than one of 50 MeV. Figs. 3 and 4 show the progressive increase in accuracy of the model. Note that the contact parameters are tuned for each value of the cutoff, using the phase shift data at 5×10^{-4} MeV (not shown) and are not tuned for each value of the energy.

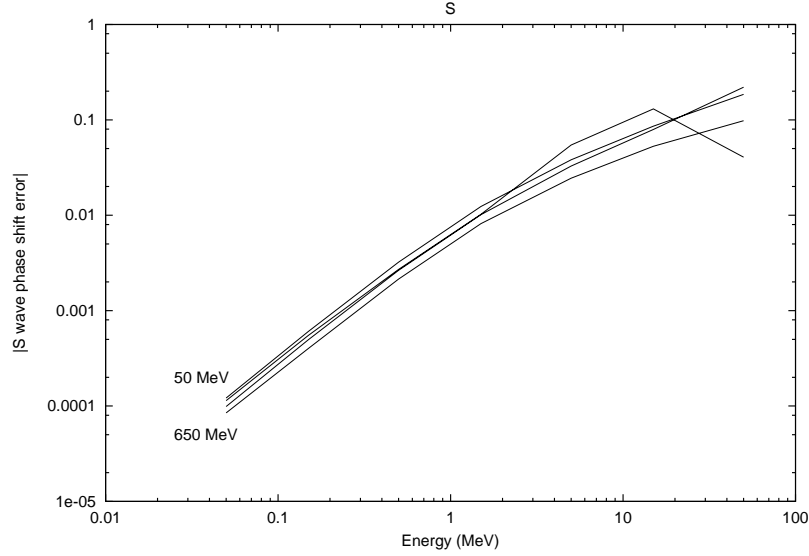


FIGURE 3. Errors in 3S_1 phase shifts for different values of the cutoff, plotted versus energy.

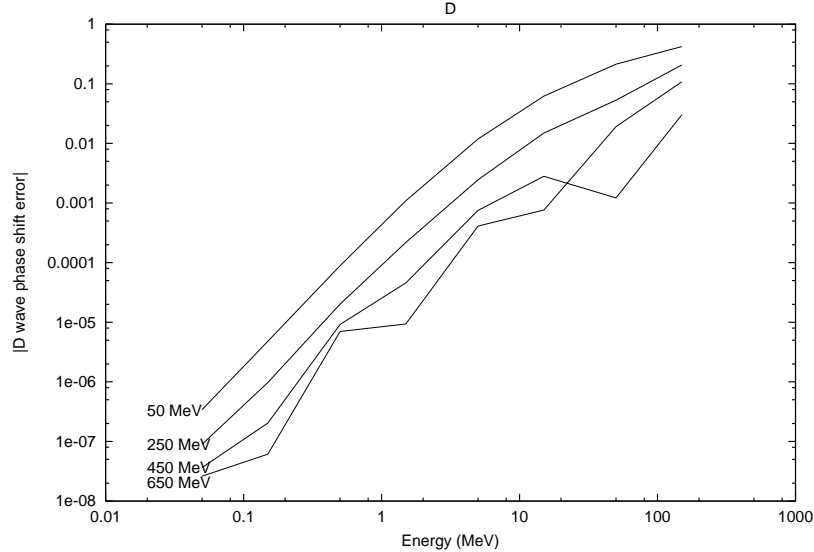


FIGURE 4. Errors in 3D_1 phase shifts for different values of the cutoff, plotted versus energy.

Notice how the error increases with increasing energy. This is due to the increasing importance of higher order terms left out of the Taylor expansion of the potential in momentum-space (Eq. 2). It indicates the energies at which physics not modeled becomes very important.

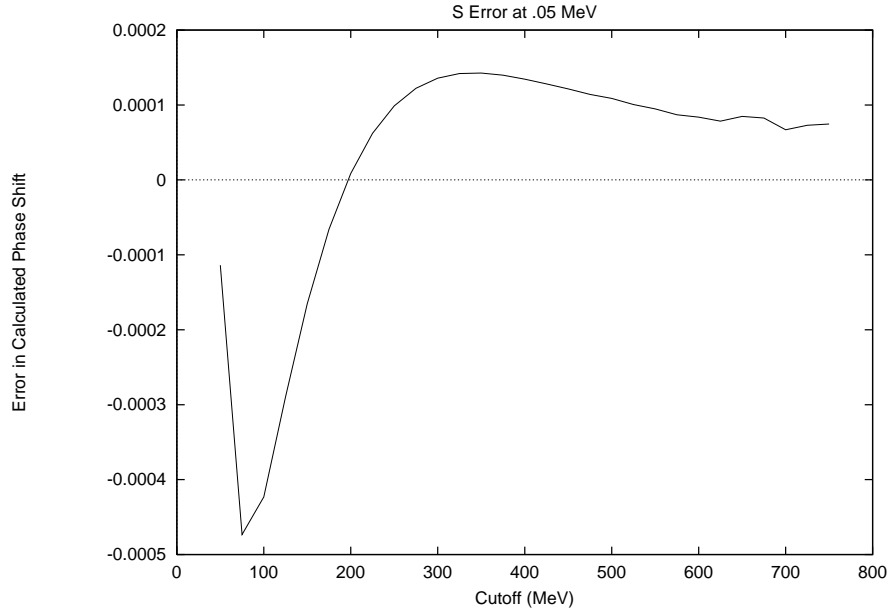


FIGURE 5. Error in the 3S_1 phase shift, plotted versus the cutoff. The model no longer increases in accuracy at $\Lambda > 600$ MeV.

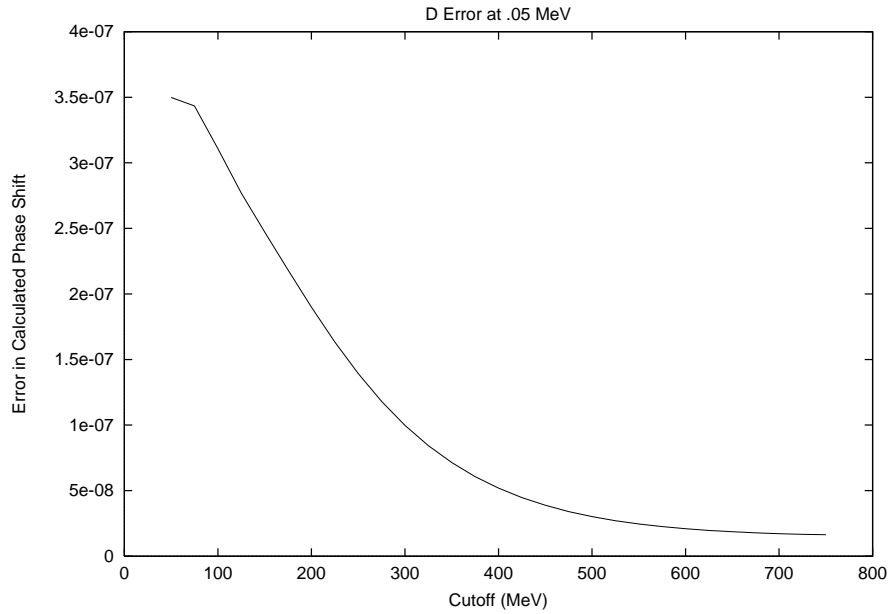


FIGURE 6. Error in the 3D_1 phase shift, plotted versus the cutoff.

As the cutoff is increased too far, the model ceases to become more accurate. Figs. 5 and 6 show the error in the 0.05 MeV phase shift versus different values of the cutoff. At cutoffs greater than 650 MeV, the error no longer decreases. Interestingly, all of the 3S_1 phase shift errors calculated have the same changing of sign at $\Lambda \approx 200$ MeV as the $E = 0.05$ MeV case shows (Fig. 5).

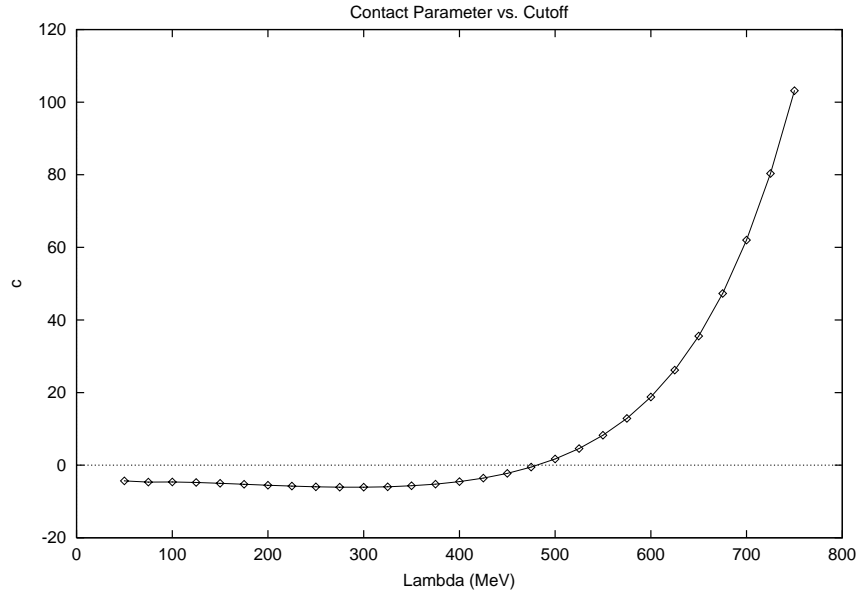


FIGURE 7. Values of the contact parameter c , tuned for different values of the cutoff.

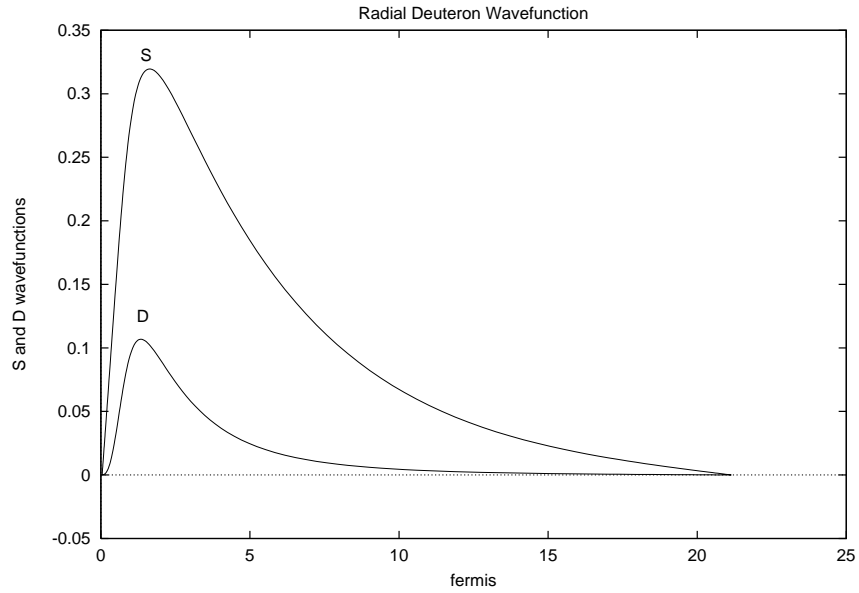


FIGURE 8. The 3S_1 and 3D_1 radial wavefunctions of the deuteron.

For larger values of the cutoff, the contact parameters must account for the incorrect physics seen by the high momentum states. The value of the contact parameter c , shown in Fig. 7 plotted versus the cutoff, starts to increase rapidly at $\Lambda \approx 600$ MeV.

The coupling of the 3S_1 and 3D_1 states produces a very loosely bound state, the deuteron. Fig. 8 shows the calculated 3S_1 and 3D_1 radial wavefunctions with $\Lambda = 500$ MeV. Fig. 9

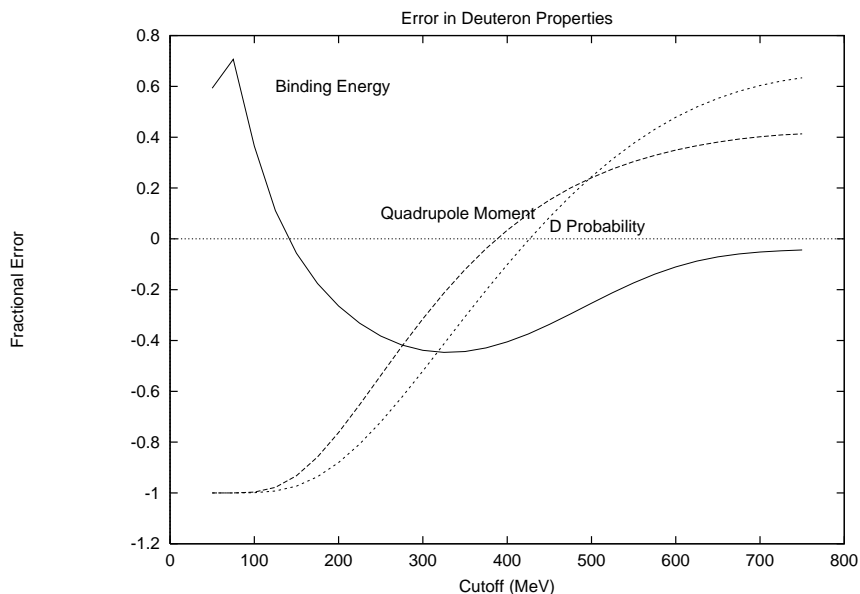


FIGURE 9. Errors in calculations of the deuteron binding energy and the deuteron’s quadrupole moment.

shows the errors in calculations of the binding energy and quadrupole moment of the deuteron, with the contact parameters tuned to phase shift data. Neglecting the axis crossings, neither of these errors decrease significantly past 600-700 MeV. The experimental values used are -2.224575 MeV for the binding energy and 0.2719 fm² for the quadrupole moment.

Conclusions

I calculated properties of neutron-proton interactions using a potential model that excludes states with momentum $> \Lambda$. I fit this model to low energy 3S_1 phase shift data for different values of Λ . The errors of the calculated 3S_1 and 3D_1 phase shifts decreased steadily at all energies with increasing Λ until $\Lambda \approx 650$ MeV, at which point the error remained fairly steady. The errors of calculations of the binding energy and quadrupole moment of the deuteron followed a similar pattern. The minimum error was about 5 % for the binding energy and 0.5 % for the quadrupole moment.

Acknowledgments

I am pleased to acknowledge the contributions of Prof. Peter Lepage, who proposed this Research Experience for Undergraduates project and guided my work. This work was supported by National Science Foundation grant PHY-9310764, and NSF REU grant PHY-9731882.

Appendix

All of the calculations integrate the radial Schrödinger equation for a coupled ${}^3S_1, {}^3D_1$ state, with contact terms and regulated potentials:

$$\left(-\frac{1}{2m_r} \frac{d^2}{dr^2} + \frac{l(l+1)}{2m_r r^2} + \begin{bmatrix} V_S & V_{S-D} \\ V_{S-D} & V_D \end{bmatrix} \right) \begin{bmatrix} \chi_S \\ \chi_D \end{bmatrix} = E \begin{bmatrix} \chi_S \\ \chi_D \end{bmatrix}. \quad (6)$$

With

$$V_S = -\alpha_\pi \nu_\Lambda(r) + \frac{c}{\Lambda^2} \delta_\Lambda^3(r) - \frac{d}{\Lambda^4} \nabla^2 \delta_\Lambda^3(r) \quad (7)$$

$$V_{S-D} = -2\sqrt{2} \alpha_\pi \nu_T(r) + \frac{d_{sd}}{\Lambda^4} \delta_T^3(r) \quad (8)$$

$$V_D = -\alpha_\pi [\nu_\Lambda - 2\nu_T(r)] \quad (9)$$

where

$$\Lambda^2 \delta_T^3(r) \equiv \frac{d^2}{dr^2} \delta_\Lambda^3(r) - \frac{1}{r} \frac{d}{dr} \delta_\Lambda^3(r) \quad (10)$$

$$\nu_\Lambda(r) = \frac{1}{2r} \left[e^{-m_\pi r} \operatorname{erfc} \left((-r\Lambda - m_\pi/\Lambda)/\sqrt{2} \right) - (r \rightarrow -r) \right] \quad (11)$$

$$\nu_T(r) = \frac{1}{m_\pi^2} \left(\nu_\Lambda'' - \frac{\nu_\Lambda'}{r} \right). \quad (12)$$

$m_\pi \approx 140$ MeV is the mass of the pion, $\alpha_\pi \approx 0.07$. c, d , and d_{sd} are the contact terms. For the above calculations, d and d_{sd} were set to zero.

Schrödinger's equation was integrated using the “odeint.c” routine found in *Numerical Recipes*.

The phase shift for a given orbital angular momentum, δ_l , is given by:

$$\tan(\delta_l) = \frac{kR j_l'(kR) - \beta_l j_l(kR)}{kR n_l'(kR) - \beta_l n_l(kR)} \quad (13)$$

where

$$\beta_l \equiv \left(\frac{r}{\chi_l} \frac{d\chi_l}{dr} \right), \quad (14)$$

with j_l and n_l the spherical Bessel functions, and $j_l'(kR)$ standing for the derivative of $j_l(kr)$ evaluated at kR .

To evaluate the phase shift, $\chi_S(r)$ and $\chi_D(r)$ were integrated from near zero to a large radius ($\gg 1/m_\pi$). The initial conditions were:

$$\begin{aligned} \chi_S(r) &= r \\ \chi_D(r) &= br^3. \end{aligned}$$

b was chosen so that

$$\begin{aligned} \chi_S(r) &\rightarrow 0 \text{ for } r \text{ large for the } {}^3D_1 \text{ shift} \\ \chi_D(r) &\rightarrow 0 \text{ for } r \text{ large for the } {}^3S_1 \text{ shift} \end{aligned}$$

To find the bound state, χ was integrated from large r to near zero with initial conditions:
 $\chi_S(r) = 0$
 $\chi_D(r) = 0$
 $\chi'_S(r) = 1$
 $\chi'_D(r)$ chosen such that $\chi_D(0) = 0$. The value of E that gives $\chi_S(0) = 0$ is the bound state energy.

The quadrupole moment is given by:

$$\frac{1}{\sqrt{50}} \int_0^\infty \chi_S(r)\chi_D(r)r^2 dr - \frac{1}{20} \int_0^\infty \chi_D^2(r)r^2 dr \quad (15)$$

Footnotes and References

1. This background is a simplified summary of parts of G.P. Lepage, *How to Renormalize the Schrödinger Equation*.
2. Partial wave analysis of the Nijmegen University group, <http://nn-online.sci.kun.nl/>.